Fire Safety Journal 141 (2023) 103929

Contents lists available at ScienceDirect

Fire Safety Journal

journal homepage: www.elsevier.com/locate/firesaf

Assessing performance of LEDSA and Radiance method for measuring extinction coefficients in real-scale fire environments

Kristian Börger [a,c], Jennifer Ellingham [b], Alexander Belt [c], Thorsten Schultze [d], Stefan Bieder [d], Elizabeth Weckman [b], Lukas Arnold [a,c,*]

[a] Computational Civil Engineering, University of Wuppertal, Wuppertal, Germany
[b] Department of Mechanical and Mechatronics Engineering, University of Waterloo, Waterloo, Canada
[c] Institute for Advanced Simulation, Forschungszentrum Jülich, Jülich, Germany
[d] Communication Systems, University of Duisburg–Essen, Duisburg, Germany

ARTICLE INFO

Keywords:
Compartment fire experiments
Smoke characteristics
Visibility
Extinction coefficient
Radiance method
LEDSA

ABSTRACT

Two photometric measurement methods (Radiance method and LEDSA) were compared against the established MIREX measurement apparatus under controlled laboratory conditions to assess their capability of measuring extinction coefficients in real-scale fires on a temporal and spatial scale. LEDSA is a tomographic technique based on direct measurements of light intensity from individual LEDs using commercially available DSLR cameras. By discretizing the domain into horizontal layers with homogeneous smoke density, values of the extinction coefficient can be computed using an inverse model based on Beer Lambert's law. The Radiance method involves measuring the contrast of light and dark areas in images and/or video footage. It was originally developed to investigate the descent of the smoke layer in high-temperature fire events. In this work, the extinction coefficient was deduced from measurements on a contrast board by a straightforward analytical approach. Both methods were shown to yield similar extinction coefficient results in line with the MIREX for an EN 54-7 TF5 n-heptane fire. The Radiance method is able to generate accurate patterns but not values for a TF2 wood smouldering fire, while LEDSA is generally able to reflect the MIREX measurement values, yet requires higher computational effort.

1. Introduction

Understanding propagation and characteristics of smoke in real-scale fires is crucial for fire safe building design. In particular, hazards arise from toxic components of fire smoke and from an impairment in visibility [1]. The latter can be estimated, for example, from numerical fire models such as the Fire Dynamics Simulator (FDS) [2] following the theory of Jin [3]. In this context, smoke density and the light extinction coefficient serve as key metrics commonly employed for quantification and model validation. Measurement techniques to assess these quantities usually rely on Beer Lambert's law [4] (see Eq. (1)), which expresses the transmission T through a homogeneous absorbing and/or scattering medium as a function of the extinction coefficient σ and the measurement path length L. This usually involves measuring the incident intensity I_0 of a light source and the transmitted intensity I in the presence of smoke from a photoelectric sensor.

$$T = \frac{I}{I_0} = \exp(-\sigma \cdot L) = \exp(-K_m(\lambda) \cdot \rho_S \cdot L) \quad (1)$$

The correlation of the smoke density ρ_S [$\mathrm{kg\,m^{-3}}$] and the extinction coefficient σ [$\mathrm{m^{-1}}$] can be established by a mass-specific extinction coefficient $K_m(\lambda)$ [$\mathrm{m^2\,kg^{-1}}$]. $K_m(\lambda)$ is reported to be almost fuel independent for smoke from well-ventilated, stoichiometric, flaming combustion [5]. However, the absorption and scattering behaviour of light by smoke particles depends on the wavelength. Widmann determined an empirical law (Eq. (2)) from a comprehensive literature review [6].

$$K_m = 4.8081 \cdot \lambda^{-1.0088} \quad (2)$$

Established devices for local smoke density measurements, such as the *Measuring InfraRed EXtinction* (MIREX) apparatus [7], rely on the Beer Lambert's law. However, it would be prohibitively expensive to use these sensors for spatially resolved smoke density measurements, e.g. for the validation of CFD (computational fluid dynamics) models. This prompted the development of the two new image-based photometric measurement methods, LEDSA (LED Smoke Analysis) [8] and the

* Corresponding author at: Computational Civil Engineering, University of Wuppertal, Wuppertal, Germany.
E-mail addresses: boerger@uni-wuppertal.de, k.boerger@fz-juelich.de (K. Börger), jennifer.ellingham@uwaterloo.ca (J. Ellingham), a.belt@fz-juelich.de (A. Belt), thorsten.schultze@uni-due.de (T. Schultze), stefan.bieder@uni-due.de (S. Bieder), beth.weckman@uwaterloo.ca (E. Weckman), arnold@uni-wuppertal.de, l.arnold@fz-juelich.de (L. Arnold).

https://doi.org/10.1016/j.firesaf.2023.103929
Received 10 July 2023; Accepted 21 August 2023
Available online 22 August 2023

Radiance method [9], which are able to determine spacially resolved extinction coefficients.

The Radiance method is a technique for measuring smoke density in real-scale fires by analysing video and/or image data. The method involves identifying contrasting light (white) and dark (black) areas in the footage to evaluate smoke progression in the compartment. The Radiance method has been tested in full-scale furniture fire experiments based on the recordings from security cameras [9]. The approach showed promise when comparing the numerical rank of smoke density results generated by human observers and from smoke density chamber [10] results for different fuels. While the Radiance method relies on capturing the contrast on externally illuminated surfaces, LEDSA is based on the direct measurement of transmission from individual light sources such as Light-Emitting Diodes (LEDs). The smoke-induced drop in light intensity can be read from sequential images recorded by consumer digital cameras. Local values of the extinction coefficient can then be deduced by an inverse modelling approach based on geometric optics and Beer Lambert's law. LEDSA was validated by local measurements of the extinction coefficient using multiple MIREX apparatus in laboratory experiments [11] similar to EN 54-7 [12] test fires. Although both methods rely on measuring intensity from image data, they originally target a different field of application. The Radiance method is intended as a robust method for analysing smoke propagation in high-temperature fire events, while LEDSA aims at the detailed analysis of smoke characteristics in controlled laboratory conditions.

Investigation into both methods under the same boundary conditions will assess the extent to which they are suitable for gauging the evolution of smoke from a fire. For this purpose, experiments were conducted involving the TF5 n-heptane flaming fire and the TF2 wood smouldering pyrolysis similar to the EN 54-7 test fires. These experiments will provide the basis for comparing the spatially resolved measurements of the extinction coefficient obtained using LEDSA and the Radiance method with the local measurements of the MIREX.

2. Experimental setup

The Heinz-Luck fire detection laboratory at the University of Duisburg–Essen, where the experiments were conducted, resembles the standardized cubic test chamber according to EN 54-7. The compartment dimensions correspond to the floor plans shown in Fig. 1, while the height-adjustable ceiling was set at 3.37 m. The laboratory is equipped with a variety of sensors including three MIREX apparatus for local measurements of smoke density at 1.6 m, 2.3 m and 3.3 m above the floor. The MIREX measures transmission within a fixed two-meter path length from a pulsed infrared diode, to a reflector, and back to a detector. The documentation indicates a peak wavelength in the $\lambda_{IR} = 880\,nm$ range [7].

In the experiments, two test fires similar to the EN 54-7 standard were examined. An n-heptane pool fire, similar to the EN 54-7 TF5 test fire, was burned in a 0.33 m × 0.33 m fuel tray. Unlike the standard, only 500 g of fuel was used here to account for the reduced ceiling height. The laboratory ventilation was activated 420 s after the n-heptane fire extinguished, until the smoke was completely exhausted. Fire TF2 corresponds to a pyrolysis-driven smouldering fire from 13 beech wood sticks, heated on a hot plate to 600 °C within 11 min. Each stick was 75 mm × 25 mm × 20 mm with a relative moisture below 5%. Moisture was determined using a wood moisture meter for building materials with a sampling range between 5% and 50%. Since the full consumption of the fuel requires a considerable amount of time, the ventilation was activated ~ 1200 s after the start of the heating phase. Within a total of 17 TF5 and 9 TF2 experiments, the arrangement of the LEDSA and Radiance method components was varied in the context of different setups, with 3–4 identical tests being carried out on each day. This study focuses on experimental setups 1 and 2, as shown in Fig. 1, encompassing one repeat set from each fuel arrangement. The results of three tests from one day were compared for both setups in order to ensure the most identical boundary conditions possible, such as the ambient and wall temperature. The experimental repeatability is evaluated on the basis of local measurements with the established MIREX system. Each of the three repeat experiments for both setups (six experiments in total) was analysed as detailed below. A comparison of the three methods is shown here with plots from a single representative experiment in each case, in order to display the emerging phenomena at the most precise level possible. Deviations of the measurements with LEDSA and the Radiance method between the individual experiments are slightly larger than those of the respective MIREX measurements, but are in the same order of magnitude. The experimental procedure for each setup is outlined in Fig. 2.

Multiple 2.4 m long RGB LED strips (LS), each featuring 144 uniformly distributed individual LEDs, served as the light sources for LEDSA. They were attached to vertically aligned aluminium columns by a thermally conductive adhesive to allow for uniform temperature dissipation. The columns were mounted on a supporting substructure with the bottom edge 0.95 m above the floor. Each of the RGB LEDs featured individual colour components with peak wavelengths measured as $\lambda_R = 632\,nm$ (red), $\lambda_G = 512\,nm$ (green), and $\lambda_B = 430\,nm$ (blue) using a dedicated LED spectrometer [13]. Each LED strip was operated in either single colour ($R \mid G \mid B$, setup 2) or multicolour (RGB, setup 1 & 2) mode. However, only the RGB strips were analysed by LEDSA for this study, since the Radiance method only allows a clear separation via the colour channels of the camera and not by the light source. Measurements using the Radiance method were made on two contrast boards (CB), each illuminated by the aforementioned LEDs on the opposite side of the room. Both boards spanned the entire height of the room with a width of 0.3 m. Each of the black and white stripes for contrast measurement were 0.1 m wide. Additionally, horizontal markers at 1 m increments from the ground served as a height reference.

Two Canon 80D cameras (*Cam-L1* and *Cam-L2* in Fig. 1) and one Canon 70D camera (*Cam-L3* in Fig. 1) were used to capture images of the LED strips. A low ISO number of 100 was selected to minimize signal noise from the camera sensor. An f/16 aperture setting was found to keep all observed LEDs in focus. The shutter speed of the cameras was set to a fixed value between 1/500 s and 1/2000 s to allow maximum use of the dynamic range of the pixels while avoiding saturation. For measurements by the Radiance method, two Sony RX0 II cameras were employed (*Cam-R1* and *Cam-R2* in Fig. 1). The cameras had a fixed focal length of 7.9 mm and a fixed aperture of f/4. Since the targeted contrast boards were not self-illuminating, the images were weakly exposed. Accordingly, the cameras needed to be operated at a high ISO value of 800 and a slow shutter speed of 1/25 s. All cameras used in the experiments were operated in manual mode to allow unbiased photometric measurements. Images were each captured at a sampling rate of 1 Hz, starting a few seconds before the ignition.

In setup 1, a general dependence of the camera height on the measured intensities and the computed extinction coefficients was investigated from the LEDSA cameras. Furthermore, two measurements each of LEDSA (*Cam-L1* on *LS-1*, *Cam-L1* on *LS-2*) and the Radiance method (*Cam-R1* on *CB-1* and *Cam-R2* on *CB-2*) are compared with the MIREX measurements. Setup 2 focuses on examining the general applicability of both methods for the TF2 test. For this purpose, the measurements of *Cam-L1* on *LS-1*, *Cam-L2* on *LS-2*, *Cam-R1* on *CB-1* and *Cam-R2* on *CB-2* are compared to the MIREX measurements.

3. Methodology

3.1. Measuring intensity from image data

Photometric measurement methods such as LEDSA and the Radiance method used in the present study are based on reading light intensity from image data. Per Eq. (1), transmittance T of the smoke, as an absorbing and/or scattering medium, is the ratio of measured

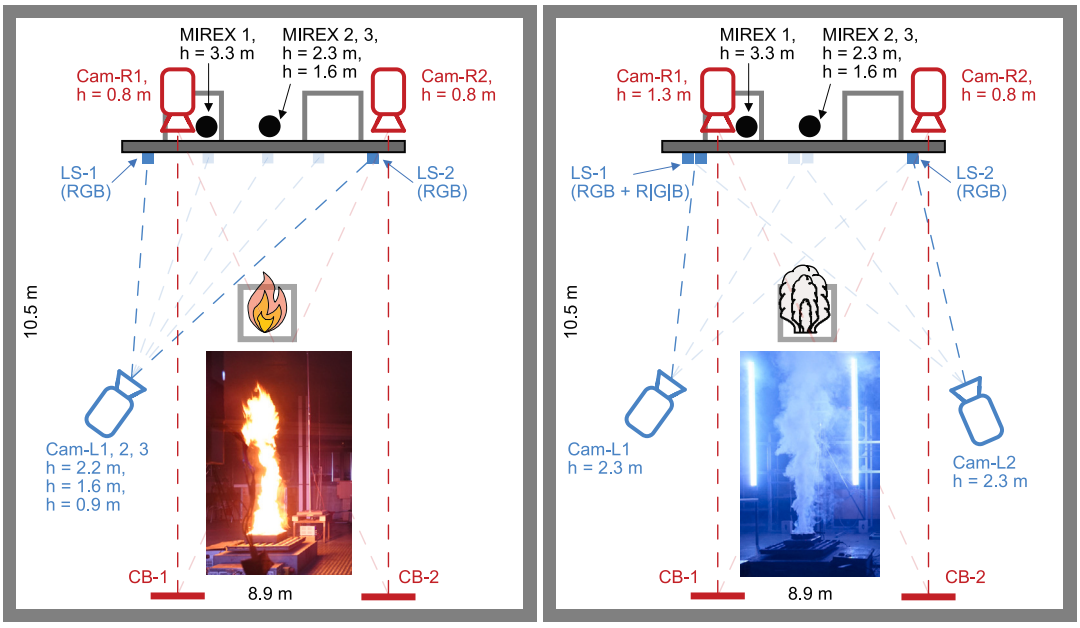

Fig. 1. Floor plans of the laboratory showing the (a) TF5 and (b) TF2 experimental setups. Camera locations were altered, while the relevant LED strips (LS) and contrast boards (CB) stayed in place.

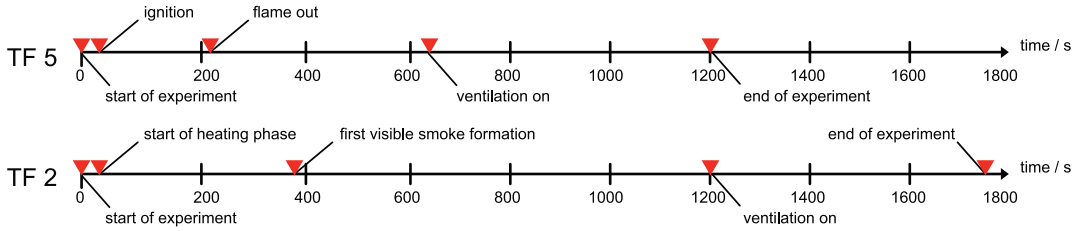

Fig. 2. Timeline of the experimental procedure.

intensity of a light source when obscured by smoke (I) and in clear condition (I_0). Hence, it corresponds to the measured luminosity of the LEDs, and the contrast measured on the contrast boards, relative to an initial value. The baseline intensities are determined from one image (Radiance method) or the average of ten images (LEDSA) taken just before the experiment, i.e. the fire, started. Hereafter, the normalized intensities will be referred to as the experimental intensity I_e.

LEDSA utilizes high-resolution image data from DSLR cameras that feature high dynamic and tonal ranges. By using RAW image files, the in-camera post-processing can be bypassed, allowing the individual red, green and blue ($R \mid G \mid B$) pixel values to be retrieved linearly from the camera's sensor readings. Conversely, the Radiance method is intended to work with relatively low-resolution image or video data, e.g. from security cameras. Such videos and JPG images are usually encoded by the camera to match human perception of luminosity, requiring a decoding scheme to be determined [9]. Accordingly, for calibration, images were taken of a standardized colour checker (see Fig. 3(a)) from each camera and setup.

The Radiance method uses the ImageJ software [14] to determine the mode $R \mid G \mid B$ pixel values from all 24 colour checker fields in each analysed image. The cameras' encoding schemes were determined by matching measured values against the listed manufacturer $R \mid G \mid B$ radiance values of the colour checker. Finally, the decoding scheme is obtained by inverting the encoding scheme. Consequently, in this work, the actual radiance normalized by the available pixel range ($255/3 = 85$), N, can be calculated from the pixel values, P, according to Eq. (3). The pixel values P are read from separate $R \mid G \mid B$ images that were extracted from the original JPG images. It takes ImageJ approximately 20 min per colour channel to separate 1200 high-resolution JPG $R \mid G \mid B$ images for analysis. ImageJ takes an additional 20 min to extract the pixel values once the images are prepared. Both tasks are carried out on a conventional desktop computer.

$$N_{R|G|B} = P/85 \tag{3}$$

Deducing the experimental intensities I_e from the image data works differently for the measurement methods. For LEDSA, I and I_0 are computed as the accumulated pixel values in the same Region Of Interest (ROI) surrounding the individual LEDs (see Fig. 3(b)). For 1200 RAW images on a desktop computer, the pixel data for all three colour channels is extracted in about 20 min from the underlying images. This needs to be done only once per camera and experiment. The ROIs are automatically detected on a reference image and centred around the maximum pixel of each LED with a fixed and predefined size (usually 20×20 pixels). The method captures small movements of the LEDs' position on the image, due to temperature dependent refraction in the compartment.

I_e according to the Radiance method is given by Eq. (4). Here, $N_{W,0}$ and $N_{B,0}$ denote the initial radiance and $N_{W,S}$ and $N_{B,S}$ denote the radiance in the presence of smoke on adjacent ROIs on the white (W) and black (B) areas, respectively. This assumes transmission losses for both surfaces are equal for every point in time. All radiance values are calculated as mean pixel values of manually selected $\sim 30\,\text{mm} \times 30\,\text{mm}$ areas corresponding to 13×13 pixel ROIs (e.g. red rectangle in

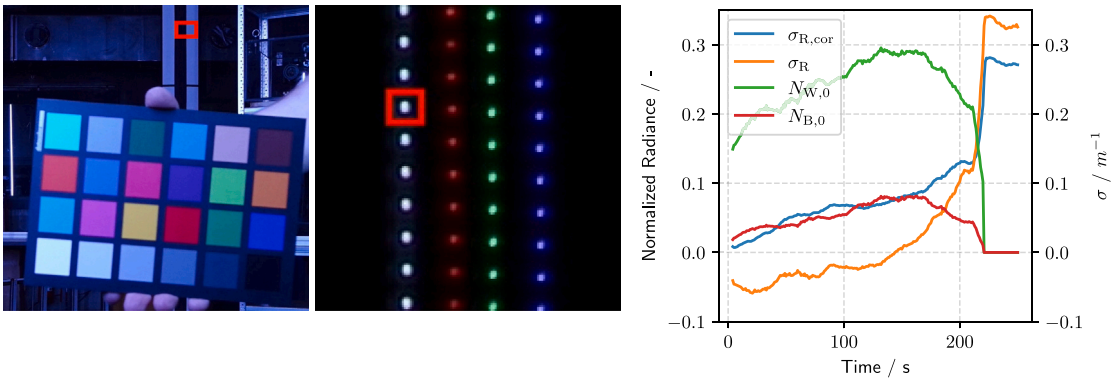

(a) (b) (c)

Fig. 3. (a) Image of the colour checker in front of a contrast board with marked ROI (red rectangle), (b) image of the LEDs as used for reading the intensities by LEDSA with marked ROI (red square), (c) example of the applied flame correction in the burning phase. (For interpretation of the references to colour in this figure legend, the reader is referred to the web version of this article.)

Fig. 3(a)). 100 ROIs were analysed between 0.18 m and 3.35 m height on each contrast board.

$$I_e = \frac{N_{W,S} - N_{B,S}}{N_{W,0} - N_{B,0}} \tag{4}$$

In the burning period of the TF5 (0 – 220 s), the flame provides additional illumination of the contrast boards. Thus, for correctness, $N_{W,0}$ and $N_{B,0}$ of the actual ROIs are substituted with the $N_{W,S}$ and $N_{B,S}$ values from the lowest ROI instead, assuming there is no smoke in the camera's line of sight. This correction reduces the error due to the additional illumination, such that the extinction coefficient is within the bounds of acceptable outcomes (i.e., positive values). Though it reduces error in all cases, this correction is most effective lower in the compartment due to proximity to the lowest measurement.

3.2. Computing extinction coefficients

The Radiance method was designed to estimate smoke density directly from the measured transmission as $1-T$ which differs from the common definition used in fire safety engineering [9]. Consequently, to generate results directly comparable to those from LEDSA and MIREX, the Radiance method was adapted to calculate extinction coefficients in the present study. Eq. (5) is a straightforward application of the Beer Lambert's law with $I_e(z_{CB})$ being the normalized intensity and $L_R(z_{CB})$ being the path length from the camera towards the observed ROI at height z_{CB} on the contrast board. This approach provides an analytical calculation of the extinction coefficient from the measured transmission under the simplified assumption that the smoke density is constant along the measurement path. The effect of flame correction as described in Section 3.1 on the extinction coefficient is illustrated in Fig. 3(c). With flame correction applied, the corrected extinction coefficient $\sigma_{R,cor}$ significantly increases over the uncorrected value σ_R.

$$\sigma_R(z_{CB}) = -\frac{\ln\left(I_e(z_{CB})\right)}{L_R(z_{CB})} \tag{5}$$

LEDSA, on the other hand, relies on a tomographic model designed to evaluate extinction coefficients by means of a spatial discretization. The fundamental assumption of the model is that the smoke density, and hence the extinction coefficients $\sigma_{L,i}$, are constant within horizontal layers i with a predefined thickness. At a certain time, the best matching set of extinction coefficients can be computed by fitting a model for the LED intensity I_m (Eq. (6)) to the actual measured intensities I_e. Here, Eq. (6) is basically the numerical integration of Eq. (1) in the camera's line of sight according to the selected layer discretization.

$$I_{m,j} = \exp\left(-\sum_{i=1}^{N_{Layers}} \sigma_{L,i} \cdot \Delta L_{L,i,j}\right) \tag{6}$$

As outlined in Fig. 4, $L_{L,i,j}$ corresponds to the travelled distance within the layer i between the camera and the LED j. The target non-linear system of equations spanned by $I_{m,j}$ and $I_{e,j}$ is solved for every image by minimizing a cost function that includes additional criteria for the optimization. This optimization requires significant computational effort, increasing almost linearly with the number of layers. The applied inverse model is described in detail in the original work [15]. Data processing on the individual time-steps can be parallelized across several CPU threads, allowing an almost lossless speed-up to be achieved. At present, a simulation based on 1200 images for one colour channel and one LED strip takes about 20 min when parallelized to 60 CPU threads of a modern HPC system. The computation of the extinction coefficients with the Radiance method is negligible due to the analytical model, which is carried out using spreadsheet software on a desktop computer.

3.3. Model uncertainties

Both the LEDSA and Radiance method approaches are subject to model-related uncertainties in computing extinction coefficients from measured intensities. In order to quantify these uncertainties and isolate them from instrumental and environmental influences, both methods are verified with synthetic data. Here, $\sigma_S(z)$ depicts the prescribed synthetic extinction coefficient of the smoke as a function of height z, assumed to be constant on a horizontal level. Supposing the camera is in line with the light source and the contrast board, the examination is simplified to a two-dimensional scale.

Smoke density, and thus the extinction coefficient, usually varies in height. σ_R, as measured by the Radiance method, therefore corresponds to the average extinction coefficient value integrated over the camera's line of sight and can be calculated analytically. For the numerical simulation with LEDSA, artificial image data is generated with 100 equidistant LEDs corresponding to the intensities that a camera at height z_C would see according to the given smoke distribution $\sigma_S(z)$. The domain is discretized into 20 equally sized layers in the range between $z = 0$ m and $z = 3$ m. Increasing the number of layers results in a higher spatial resolution, but does not yield better results as it reduces the amount of information for each layer for the optimization. A sensitivity analysis in this regard was conducted in the original work [15].

Fig. 5 shows the resulting extinction coefficients by LEDSA (σ_L) and the Radiance method (σ_R) that would result from a constant, linear, and quadratic profile of σ_S with the cameras being at $z_C = 1$ m and $z_C = 2$ m. Positions of the cameras and light sources used in this example are chosen for simplicity and to highlight comparisons, and thus differ from the actual experiments.

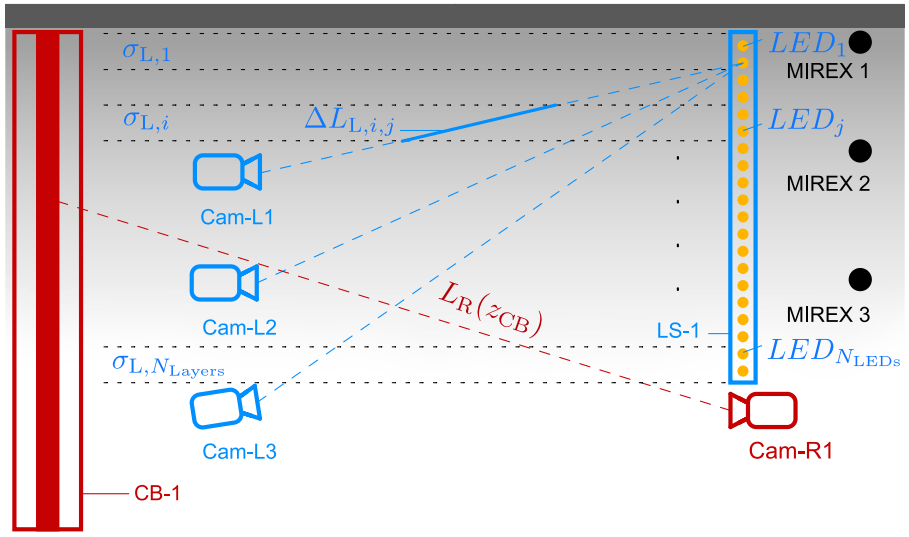

Fig. 4. Cross-sectional view through the laboratory showing the arrangement of the cameras as well as a contrast board (*CB-1*) and an LED strip (*LS-1*) in setup 1. $L_{L,i,j}$ is the path length in layer i in the camera's line of sight to LED j. $L_R(z_{CB})$ is the full sensing path for the Radiance method from the camera to a specific ROI at height z_{CB} on the contrast board.

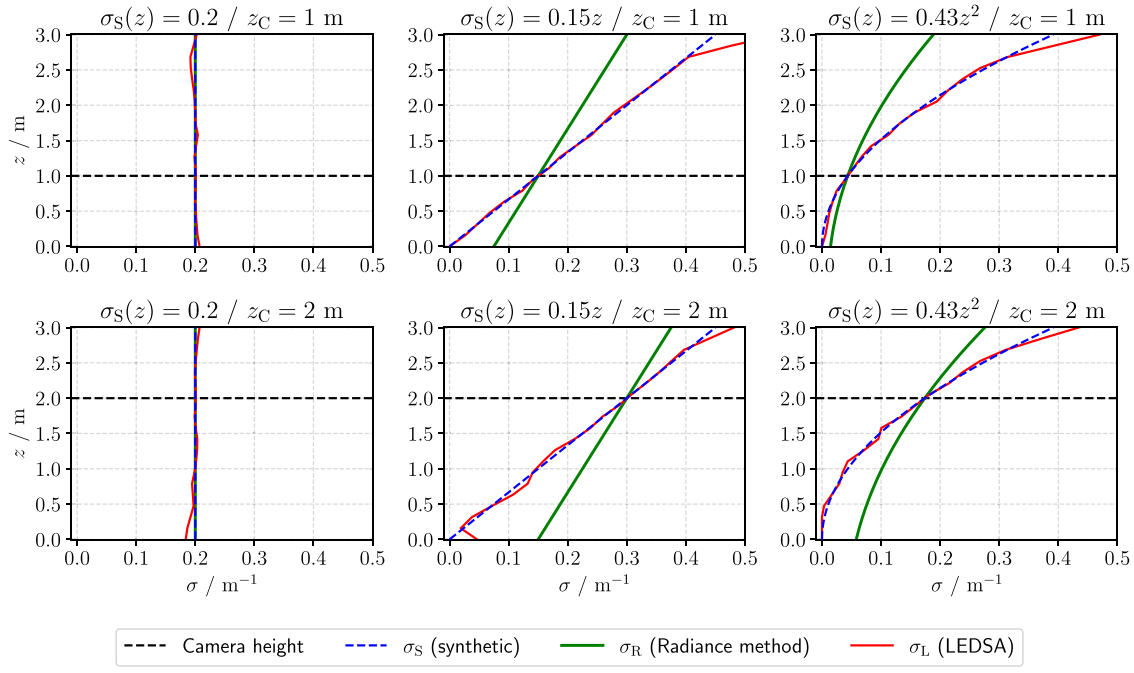

Fig. 5. Example based on synthetic data, showing the model-conditioned systematic and numerical deviations between the real extinction coefficient σ_S and as measured by LEDSA (σ_L) and the Radiance method (σ_R). (For interpretation of the references to colour in this figure legend, the reader is referred to the web version of this article.)

The LEDSA extinction coefficient σ_L closely follows the synthetic extinction coefficient σ_S for all three profiles, with the only notable deviations (up to $\sim 0.1\,\mathrm{m}^{-1}$) in the top two or bottom two layers. σ_R accurately estimates the constant profile of σ_S while for the linear and quadratic profiles, it matches at the camera height but increasingly deviates with $\Delta z = |z_C - z|$. Accordingly, correct measurement of the extinction coefficient by the Radiance method as presently formulated should only be possible at the height of the camera or when the smoke density is perfectly uniform across the sensing range. With smoke density increasing upward, the measured value gets overestimated below the camera and underestimated above the camera. It should be noted, that this may be due to the fact, that Eq. (5) is providing the extinction values with regard to the target position on the contrast board (z_{CB}). Although LEDSA aims at computing the real extinction coefficients, it is subject to numerical uncertainties. As noted, deviations from σ_S arise especially in the peripheral areas. A steeper viewing angle from the camera results in shorter sensing ranges, so the edge layers are less weighted by the cost function. The presented model can only give a broad outline of the model-related uncertainties and therefore misses some crucial parameters related to the instrumental and environmental effects.

3.4. Instrumental and environmental uncertainties

The uncertainties in the experimental determination of the extinction coefficient can be attributed to both the instrumentation and the experimental boundary conditions. Besides intrinsic noise, both the detector and the light sources can be systematically affected by extrinsic influences. As ambient temperature increases, the emitted intensity

of LEDs generally decreases exponentially, depending on the type of semiconductor and thus the colour of the LED [16]. The uncertainty from the internal thermally-induced drift was reduced by turning on the LEDs at least 20 min before the experiments until a constant operating temperature of about 40 °C was reached on the LED surfaces. The temperature was measured by exposed thermocouples that were attached to the LEDs below the thermally-insulated silicone coating. The influence of external thermal stress on the measurement accuracy is discussed in [11]. Changes in LED lighting inherently influence Radiance method results. However, no advantageous correction for the LED light impact could be found, so no correction for this effect was applied. All cameras were housed in PMMA and glass boxes, and should therefore remain insensitive to the convective effects of hot smoke. The MIREX incorporates a reference receiver to compensate for thermal drift and ageing of the light source. Temperature influence is likely to be relevant only for TF5 tests, since no significant increase in temperature was measured in the laboratory for the TF2 tests. For the application in high-temperature tests, it might be advisable to place the cameras and LEDs in cooled boxes or even outside the compartment. In this context, the effects of the respective protective layers, such as glass panes, on the light spectrum may have to be taken into account.

Deposition of smoke particles on the instrumentation increasingly distorts the measured light intensity during the course of the experiment. This particularly applies to the MIREX lenses and detectors, LEDs, cameras, and contrast boards close to the ceiling where smoke density is the highest. Comparing the initial extinction coefficient and the asymptotic values post ventilation, this soot deposit impact increases at higher measurement points for all three methods (see Figs. 7, 8). As expected, the effect is negligible for white smoke, such as in the case of TF2, since the particles have an absorbance much lower than the scattering effect [17]. The MIREX, as well as both of the introduced novel measurement methods, can currently only measure light extinction as a whole. However, LEDSA also may potentially provide the means to derive refraction and scattering phenomena from the detected shape and position of the individual LEDs in the future. The original paper also presents an approach to these issues [15].

Since the flame is not shielded from the experimental setup, it poses an additional light source that can distort the measured transmission in the TF5 tests. This effect increases if the reference source for the light measurement has a comparatively low intensity, as for the contrast boards. It can be quantified by measuring the light intensity gradient in an area not affected by smoke obscuration while the fire goes out. Corresponding to the emitted light spectrum of a diffuse n-heptane flame, the effect should be greatest on the red colour channel of the cameras. The intensity drop on an LED near the ground was observed to be less than 2% for *Cam-L3*. As shown in Fig. 3(c), the effect is much higher for Radiance method results, but was significantly reduced with the flame light correction applied. Furthermore, environmental influences affecting the smoke stratification can have a significant impact on the measurement accuracy. LEDSA assumes the smoke density to be homogeneous on a horizontal level. This assumption is likely to be a good approximation for the MIREX, as it covers a comparatively low measuring distance. In [11], it was shown that the computed extinction coefficients by LEDSA show notable deviations as the camera is shifted horizontally. However, the effect was not observed until the flame was extinguished. Most likely, the descent of the smoke layer in the post flame phase is affected by different wall temperatures of the laboratory.

3.5. Influence of camera height

Measuring the intensities of the corresponding light sources provides the raw data for calculating the extinction coefficient using LEDSA and the Radiance method. Since the smoke is usually not homogeneously distributed over the observed domain, the intensity measurement (I_e) is significantly affected by the position of the camera in the smoke laden environment. The cameras *Cam-L1* - *Cam-L3* in setup 1 were placed at the same location, but at different heights, so the above-mentioned influences can be demonstrated from comparing the respective normalized intensities. Fig. 6 depicts the normalized LEDSA intensities for a TF5 test from all 144 LEDs of the same strip (*LS-1*) as a function of time and height. In the burning period, the descending smoke layer can be observed for each camera, which is characterized by distinctly lower intensities. With maximum depth around the time of flame out, the smoke layer slightly retreats as mixing occurs with ambient air, and then rapidly draws back when the ventilation is turned on.

Comparing between cameras, the measured intensities decrease across all LEDs when captured from an elevated perspective. Despite a considerably higher optical path, the maximum drop on the top LED, for example, is 77% for *Cam-L1* and 65% for *Cam-L3*. This difference indicates the smoke density increases with height above floor level. Data from *Cam-L3* further reveals that the camera remains outside the smoke until about 200 s after ignition. This allows for a rough estimate on the smoke layer to drop to about 1.5 m. LEDSA is capable of dealing with different camera positions and yield similar extinction coefficients, see Section 3.3. It is expected that the intensities measured by the Radiance method will also be influenced by camera height, though quantifying the impact on the resulting extinction coefficients is future work.

4. Results and discussion

4.1. Evaluation of repeatability using established measurement methods

The overall repeatability of the experiments can best evaluated based on the MIREX readings, as these are expected to provide the lowest measurement uncertainty (see Fig. 7).

For the TF5 tests, the mean extinction coefficient rapidly rises to $0.24\,m^{-1}$, $0.16\,m^{-1}$ and $0.10\,m^{-1}$ for the top, middle and lower MIREX until around flame out at $\sim 220\,s$. After that, the smoke layer can be observed to gradually settle down, which is evident from a decrease in the extinction coefficient at the top MIREX and an increase at the lower ones. From $\sim 400\,s$ a steady drop occurs on all MIREX, followed by a spike when the ventilation is turned on at $\sim 620\,s$ which results from the smoke being extracted close to the ceiling. For the TF2, the top MIREX rises to $0.85\,m^{-1}$ $\sim 900\,s$ after the beginning of the heating phase before declining at a similar rate. The top MIREX decreases more rapidly after the fans are turned on $\sim 1200\,s$. The higher extinction coefficients, relative to the TF5 tests, may be the result of more or different particles and will be the subject of future analysis. The middle and lower MIREX indicate a much lower extinction coefficient, with a maximum peak of $0.28\,m^{-1}$ and $0.20\,m^{-1}$ respectively at $\sim 1300\,s$.

The standard deviation results indicate good reproducibility of the TF5 experiments. Due to thermal dynamics in the burning phase, smoke propagation here is essentially driven by forced convection. With the fire extinguished and the buoyancy subsiding, the environmental boundary conditions start having a stronger effect. The TF2 tests, in contrast, feature considerably higher standard deviations, and thus lower reproducibility. As pyrolysis of the wooden sticks entails negligible heat release, the resulting smoke is driven by low buoyancy. Furthermore, the process is affected by inhomogeneous material properties and certain residual moisture.

4.2. LEDSA and radiance method with a flaming fire

Alignment of the extinction coefficients derived from LEDSA and the Radiance methods, compared to the MIREX results, indicates that both methods are generally capable of assessing smoke density in a temporal and spatial context. Fig. 8 shows the extinction coefficient results for a representative TF5 test at the three MIREX heights (3.3 m, 2.3 m, 1.6 m). The red camera channel is analysed for the LEDSA and Radiance method results in this work since red light is closest to infrared light of

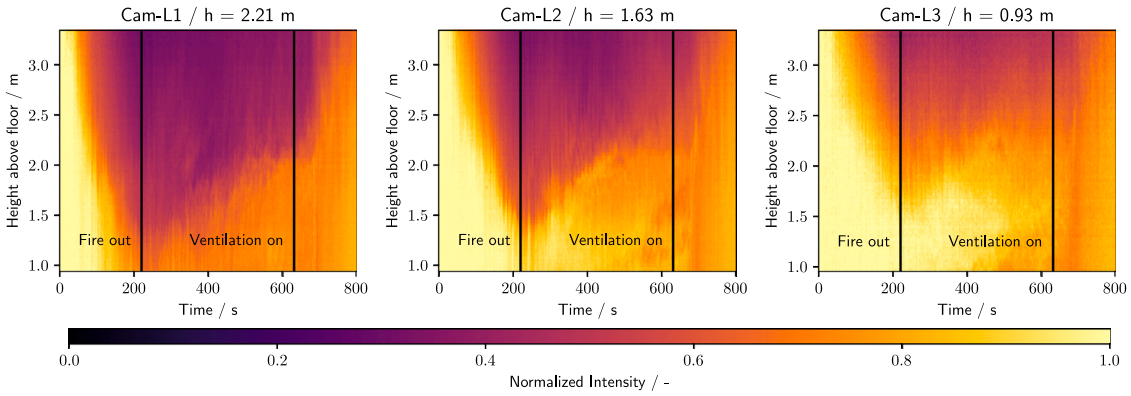

Fig. 6. Intensity as a function of height and time, measured on a single RGB LED strip. Cameras are located in the same position in the laboratory at heights of 2.21 m, 1.63 m and 0.93 m above the floor. Data is shown for the red colour channel of the cameras. (For interpretation of the references to colour in this figure legend, the reader is referred to the web version of this article.)

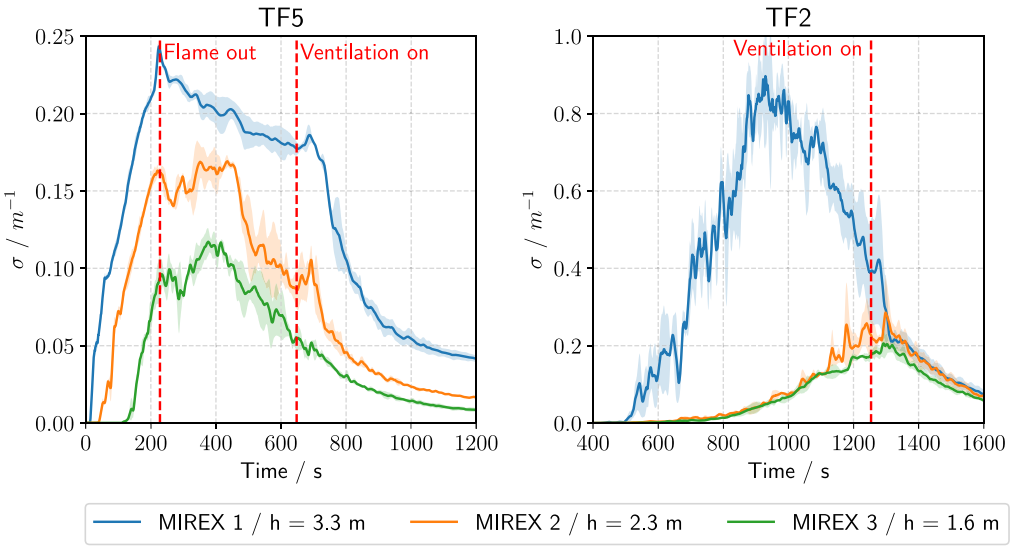

Fig. 7. Mean value (solid lines) and ± 1 standard deviation (shaded areas) of the extinction coefficient of 3 TF5 and 3 TF2 tests, smoothed by a 10 s moving average. Measurements were taken by MIREX devices at heights 1.6 m, 2.3 m and 3.3 m above the floor. (For interpretation of the references to colour in this figure legend, the reader is referred to the web version of this article.)

the MIREX. For better comparability, the MIREX extinction coefficient measurements were linearly scaled by the factor $K_{m,(R)}/K_{m,(IR)}$ according to Eq. (2) with respect to the peak wavelength of the red LEDs (λ_R = 632 nm) and the MIREX (λ_{IR} = 880 nm), respectively. However, this scaling factor provides only a coarse approximation since the LEDs do not emit monochromatic light and the emitted spectrum does not correspond to the response spectrum of the cameras.

In general, the LEDSA and Radiance method extinction coefficients align with the MIREX results, while LEDSA seems to match the smoke dynamics captured by the MIREX more precisely. However, the LEDSA results display fluctuations at the peripheral regions, as expected based on the numerical approach discussed in Section 3.3. Indeed, the Radiance method results are much closer to MIREX and LEDSA results than was expected based on the systematic discrepancies seen in comparison to synthetic data. A major influence that could not be accounted for in the prediction is that the illumination of the contrast boards is reduced via smoke-induced attenuation of the incident light. Quantifying this influence will be the subject of future work.

During the burning period, the Radiance method values fall below the MIREX and LEDSA results at all three heights. This difference was reduced by the applied flame correction, discussed in Section 3.1. After flame out, the Radiance method results are neither consistently above nor below LEDSA and MIREX results. After peaking at the same level around flame out, slightly lower values are measured by *Cam-L1* on *LS-2* and *Cam-R2* on *CB-2* than by *Cam-L1* on *LS-1* and *Cam-R1* on *CB-1* at each of the three heights, respectively. This may indicate an actual inhomogeneity of the smoke stratification. Similar deviations between measurements have already been observed in previous TF5 experiments with LEDSA [11]. Here, a centred LED strip was seen by two cameras to the left and right of the set-up at approximately the same distance.

Both methods show considerable deviations in the measured extinction coefficients compared to the MIREX at the height of 1.6 m after flame out. This can most likely be attributed to this area being in the smoke/ambient air transition zone.

Fig. 9 depicts a height profile of the extinction coefficients from the measurements of the MIREX, the *Cam-R1* and all three LEDSA cameras of the same representative TF5 experiment in the burning phase (100 s) and after flame out (300 s and 500 s).

At 100 s, all three measurements indicate minimal smoke below 1.8 m. LEDSA closely matches the MIREX results, with no significant effect of the height of the camera evident in the tomographic model. The results are underestimated by the Radiance method and feature a

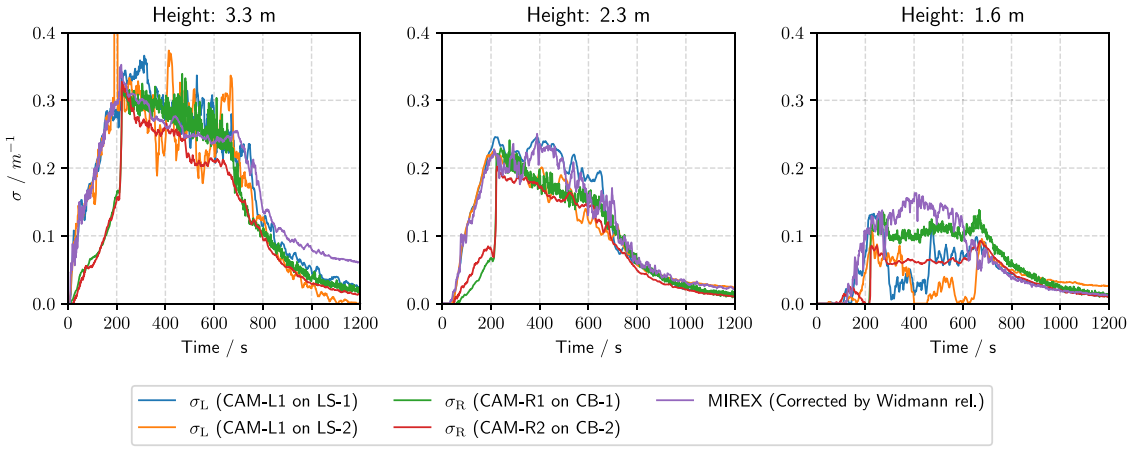

Fig. 8. Extinction coefficients of the MIREX, LEDSA and Radiance method at 3.3 m, 2.3 m and 1.6 m height for the TF5 test, smoothed by a 10 s moving average. The MIREX results are scaled by Eq. (2) according to the wavelength of the red LEDs. (For interpretation of the references to colour in this figure legend, the reader is referred to the web version of this article.)

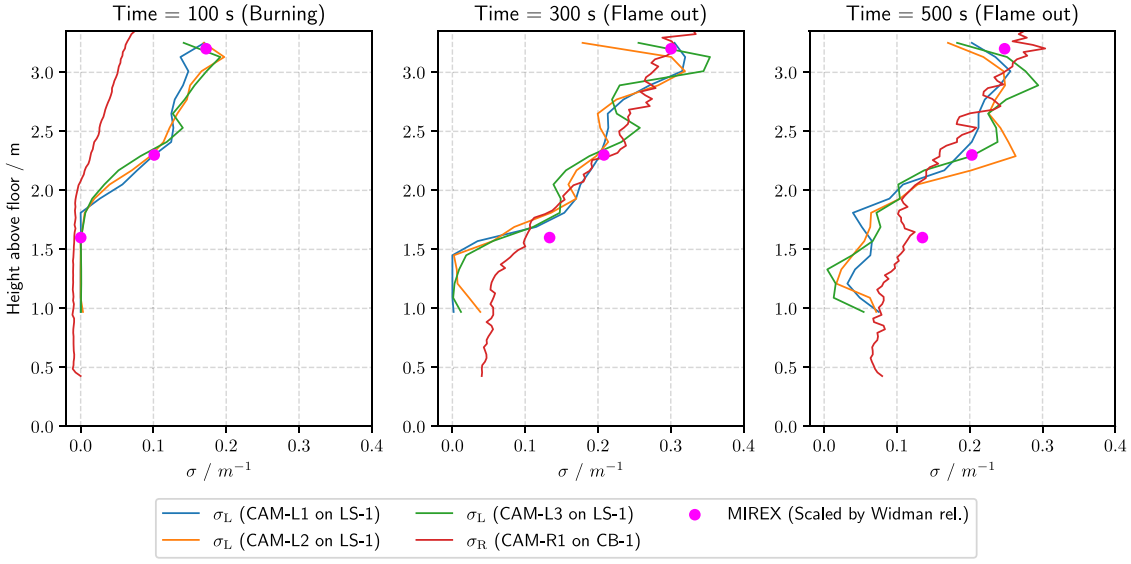

Fig. 9. Extinction coefficients of the MIREX, LEDSA and Radiance method for the TF5 test as a function of height at different times. The MIREX results are scaled by Eq. (2) according to the wavelength of the red LEDs. (For interpretation of the references to colour in this figure legend, the reader is referred to the web version of this article.)

differently shaped profile. At 300 s and 500 s LEDSA and the Radiance method are in good agreement with the MIREX results, and each other, above 1.5 m. Below 1.5 m, there appears to be minimal smoke present in the post-flame, pre-ventilation period. Though the LEDSA and Radiance methods results differ in this region with values between ~ 0 and 0.1 m^{-1}. It is likely that the LEDSA results at 300 s indicate a distinct smoke boundary at 1.5 m while the Radiance method captures a more blurred transition here.

4.3. LEDSA and radiance method with a smouldering fire

Despite being based on experiments involving flaming combustion, Eq. (2) appears to be at least a good approximation for scaling the TF2 MIREX results according to the wavelength of the red LED. Fig. 10 shows extinction coefficient results for a representative TF2 test at the three MIREX heights (3.3 m, 2.3 m, 1.6 m). Again, the red channel is used from the LEDSA and Radiance method results to minimize MIREX data scaling error.

Extinction coefficients measured by LEDSA at heights 2.3 m and 1.6 m closely match the MIREX results, while a significant overestimation by the Radiance method can be observed. The head-on exposure of the contrast boards by the LEDs is likely to cause a significant amount of the light to be back scattered from the smoke particles. This influence results in a substantial drop in the contrast on the black and white areas, thus, in an underestimation of the transmittance and overestimation of the extinction coefficient. At 3.3 m, the Radiance method results fall below the MIREX and LEDSA results. However, considerable noise impedes the comparison at the uppermost measurement point. The noise is likely to be related to both the lighting inside the laboratory and the smoke characteristics. As with the TF5 tests, the LEDSA results display more fluctuations in value at the high locations, which is in line with the predicted model uncertainties at the boundary layers, as described in Section 3.3.

5. Conclusions and outlook

In this paper, two photometric measurement methods for the analysis of smoke density were presented and compared under known laboratory conditions. The novel LEDSA and Radiance methods, involve low-cost setups and, unlike the established MIREX apparatus, target spatially and temporally resolved measurements of light extinction

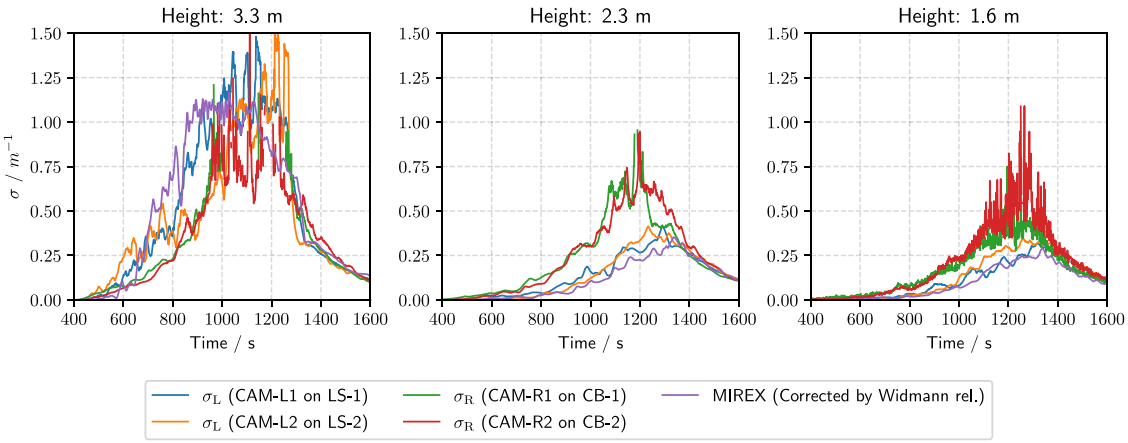

Fig. 10. Extinction coefficients of the MIREX, LEDSA and Radiance method at 3.3 m, 2.3 m and 1.6 m height for the TF2 test, smoothed by a 20 s moving average. The MIREX results are scaled by Eq. (2) according to the wavelength of the red LEDs. (For interpretation of the references to colour in this figure legend, the reader is referred to the web version of this article.)

coefficients. LEDSA involves measuring transmission from dedicated light sources such as LEDs by high resolution DSLR cameras. At present, the method is designed for laboratory-scale measurements, rather than for field applications, especially in high-temperature environments. The current (unoptimized) version of LEDSA, requires significant computational effort, practically requiring parallel computation on an HPC (High Performance Computing) system for computing the extinction coefficients. Data analysis using the Radiance method can be performed on a desktop computer and may therefore allow for real-time measurements in the future. The method was designed to work with low-cost cameras, with resolution proportional to the spatial domain of interest. Examining smoke propagation typically only requires multiple adjacent contrasting light and dark areas within the image which are illuminated by ambient light. However, to determine extinction coefficients comparable with the LEDSA results, contrast boards illuminated by the above-mentioned LEDs were used for the contrast measurements in the conducted experiments.

It was demonstrated that both methods are capable of capturing the dynamics of black smoke such as emerges from the investigated TF5 n-heptane fire. On a temporal and spatial scale, they show good agreement with local measurements from the established MIREX system. In case of white smoke from the TF2 wood smouldering pyrolysis fire, the Radiance method can provide an indication of the smoke density patterns but not accurate measured values under the given experimental conditions. This can likely be attributed to considerable backscattering of the incident light on the smoke particles, resulting in poor contrast between the light and dark areas on the images. LEDSA, on the other hand, can reproduce the MIREX measurements to a large extent. However, in the peripheral areas of the measurement range, the method partly exhibits increased uncertainty and noise due to the numerical model.

The Radiance method showed much better accuracy than expected due to the model uncertainty revealed by a synthetic data set. Real experimental data analysis indicates that the model uncertainties may be competing with factors due to lighting conditions. A more in depth analysis and quantification of influences on the LEDSA and Radiance methods will be the subject of future work. Analysis of additional TF2 and TF5 experiments will aid in better accuracy quantification. This includes analysis based on the remaining colour channels of the cameras, as well as investigation of different experimental setups.

Declaration of competing interest

The authors declare that they have no known competing financial interests or personal relationships that could have appeared to influence the work reported in this paper.

Data availability

Data will be made available on request.

Acknowledgements

The authors gratefully acknowledge the financial support of the German Federal Ministry of Education and Research and the Natural Sciences and Engineering Research Council of Canada Grant number: RGPIN-2022-03715. The extensive LEDSA computations were performed largely on the high-performance computer system funded as part of the CoBra project, Germany with the grant number 13N15497.

References

[1] David A. Purser, Jame L. McAllister, Assessment of hazards to occupants from smoke, toxic gases, and heat, in: Morgan J. Hopturley (Ed.), SFPE Handbook of Fire Protection Engineering, fifth ed., Springer, ISBN: 9781493925643, 2016, http://dx.doi.org/10.1007/978-1-4939-2565-0.

[2] Kevin McGrattan, Simo Hostikka, Jason Floyd, Randall McDermott, Marcos Vanella, Fire Dynamics Simulator User's Guide – Version 6.7.9, 2022, http://dx.doi.org/10.6028/NIST.SP.1019.

[3] Tadahisa Jin, Visibility through Fire Smoke (I), Bull. Jpn. Assoc. Fire Sci. Eng. 19 (2) (1970) 1–8, http://dx.doi.org/10.11196/kasai.19.2.1.

[4] M. Pierre Bouguer, William Edgar Knowles Middleton, Optical Treatise on the Gradation of Light. Translated, with Introduction and Notes, By WE Knowles Middleton, University of Toronto Press, 1961.

[5] George W. Mulholland, Carroll Croarkin, Specific extinction coefficient of flame generated smoke, Fire Mater. 24 (5) (2000) 227–230, http://dx.doi.org/10.1002/1099-1018(200009/10)24:5<227::aid-fam742>3.0.co;2-9.

[6] John F. Widmann, Evaluation of the planck mean absorption coefficients for radiation transport through smoke, Combust. Sci. Technol. 175 (12) (2003) 2299–2308, http://dx.doi.org/10.1080/714923279.

[7] Cerberus, Ionization measuring chamber MIC Extinction measuring equipment MIREX, Technical Description, 1992, (available on request).

[8] Kristian Börger, Alexander Belt, Lukas Arnold, LEDSA: A Python package for determining spatially and temporally resolved extinction coefficients of fire smoke, J. Open Source Softw. (2023) Submitted to JOSS.

[9] Jennifer Ellingham, Measuring Smoke Evolution at Full-Scale with Video Recordings (Master's thesis), University of Waterloo, 2021, URL https://hdl.handle.net/10012/16818.

[10] International Organization for Standardization, ISO 5659, Plastics — Smoke generation, Part 2: Determination of optical density by a single-chamber test, 2006.

[11] Kristian Börger, Alexander Belt, Thorsten Schultze, Lukas Arnold, Remote sensing of the light-obscuring smoke properties in real-scale fires using a photometric measurement method, Fire Technol. (2023) http://dx.doi.org/10.1007/s10694-023-01470-z.

[12] The European Committee for Standardization, EN 54, Fire Detection and Fire Alarm Systems, Part 7: Smoke Detectors Point Detectors Using Scattered Light, Transmitted Light or Ionization, 2000.

[13] Gigahertz Optik BTS256-LED Tester, Technical Report.

[14] M.D. Abramoff, P.J. Magelhaes, S.J. Ram, Image processing with ImageJ, Biophotonics Int. 11 (7) (2004) 36–42.
[15] Lukas Arnold, Alexander Belt, Thorsten Schultze, Lea Sichma, Spatiotemporal measurement of light extinction coefficients in compartment fires, Fire Mater. (2020) http://dx.doi.org/10.1002/fam.2841.
[16] E. Fred Schubert, Light-Emitting Diodes, second ed., Cambridge University Press, New York, 2006, http://dx.doi.org/10.1017/CBO9780511790546.
[17] Edward M. Patterson, R.M. Duckworth, C.M. Wyman, E.A. Powell, J.W. Gooch, Measurements of the optical properties of the smoke emissions from plastics, hydrocarbons, and other urban fuels for nuclear winter studies, Atmos. Environ. A. 25 (11) (1991) 2539–2552, http://dx.doi.org/10.1016/0960-1686(91)90171-3.